



THE UNIVERSITY *of* EDINBURGH

Edinburgh Research Explorer

Technoeconomic evaluation of multiple MSMPR crystalliser configurations for continuous cyclosporine crystallisation

Citation for published version:

Diab, S & Gerogiorgis, D 2017, 'Technoeconomic evaluation of multiple MSMPR crystalliser configurations for continuous cyclosporine crystallisation' *Organic Process Research & Development*, vol. 21, no. 10, pp. 1571.

Link:

[Link to publication record in Edinburgh Research Explorer](#)

Document Version:

Publisher's PDF, also known as Version of record

Published In:

Organic Process Research & Development

Publisher Rights Statement:

GOLD OPEN ACCESS ARTICLE

General rights

Copyright for the publications made accessible via the Edinburgh Research Explorer is retained by the author(s) and / or other copyright owners and it is a condition of accessing these publications that users recognise and abide by the legal requirements associated with these rights.


Take down policy

The University of Edinburgh has made every reasonable effort to ensure that Edinburgh Research Explorer content complies with UK legislation. If you believe that the public display of this file breaches copyright please contact openaccess@ed.ac.uk providing details, and we will remove access to the work immediately and investigate your claim.





Technoeconomic Evaluation of Multiple Mixed Suspension-Mixed Product Removal (MSMPR) Crystallizer Configurations for Continuous Cyclosporine Crystallization

Samir Diab and Dimitrios I. Gerogiorgis*

Institute for Materials and Processes (IMP), School of Engineering, University of Edinburgh, The King's Buildings, Edinburgh, EH9 3FB, United Kingdom

ABSTRACT: Continuous crystallization using Mixed Suspension-Mixed Product Removal (MSMPR) crystallizers has been demonstrated as a feasible method for implementing continuous separations in pharmaceutical manufacturing processes. This work conducts a steady-state process modeling and simulation study of the continuous cooling crystallization of cyclosporine, comparing processes with and without solids recycle for their technoeconomic viability. The model describes population balance equations, crystallization kinetics, and process mass balances to compare attainable crystallization and plantwide yields of different process configurations. Total cost components using an established economic analysis methodology are compared for varying numbers of crystallizers, operating temperatures, total crystallizer cascade residence times and API feed concentrations. Economic analyses and the calculation of normalized cost components with respect to total crystallizer volumes identify the process without recycle as the most economically viable option, achieving the lowest total costs and low *E*-factors for pharmaceutical processes. The sensitivity of total costs to the selected total residence times for economic analyses highlights the need for rigorous comparison methodologies. This work identifies the need for technoeconomic optimization studies of continuous crystallization processes to establish the optimal design of manufacturing campaigns prior to further development.

1. INTRODUCTION

Continuous pharmaceutical manufacturing (CPM) has been established as a promising new paradigm with the potential for significant technoeconomic benefits for the pharmaceutical industry.¹ While the current batch manufacturing methods have advantages such as specific product recall, flexible equipment usage and well-established analytical methods for quality control, they imply large material inventories, significant intermediate storage and poor mixing and heat transfer efficiencies.²⁻⁴ Various demonstrations of continuous flow syntheses,⁵⁻⁷ product formulation stages⁸ and fully end-to-end production campaigns⁹⁻¹³ show the initiative of academic and industrial researchers to facilitate the transition toward continuous methods. Despite these efforts, a stagnancy against widespread adoption of CPM exists due to investments in batchwise infrastructures and limited technological expertise in continuous pharmaceutical processes compared to current techniques.^{14,15} Furthermore, the limited number of demonstrated continuous pharmaceutical purifications and separations presents a bottleneck to realizing end-to-end CPM.

Crystallization is an essential unit operation in pharmaceutical manufacturing prior to downstream processing. Batch crystallization techniques are currently dominant in the pharmaceutical industry; however, batch-to-batch variability is an issue for the strict purity regulations placed upon pharmaceutical products.¹⁶ Continuous crystallization operates under steady-state conditions, allowing higher reproducibility and better control of important crystal properties such as the purity and the size distribution, which directly affect the bioavailability of the product; however, as continuous processes do not discharge at equilibrium, they tend to achieve lower yields than batch crystallizations.¹⁷ Systematic investigation of

continuous crystallization processes for pharmaceutical manufacturing is required to realize the attainable benefits compared to existing batch methods.

Continuous crystallizer designs applicable for the pharmaceutical industry are categorized as plug flow (PF), oscillatory baffled crystallizers (OBCs) or Mixed Suspension-Mixed Product Removal (MSMPR) crystallizers. PF crystallizers are suited to systems with fast crystal growth kinetics and short residence times and can attain narrow crystal size distributions,¹⁸ but fouling and clogging in narrow tube diameters is an important technical issue.¹⁹ OBCs are another emerging technology, which enhance heat and mass transfer, but have issues handling streams with high solid loadings.²⁰ Various experimental and modeling studies in OBCs have been conducted for the estimation of crystallization kinetics, proof-of-concept demonstrations and design and optimization processes.²¹⁻²⁶

MSMPR crystallizers are idealized stirred tank designs better suited for systems with slower crystallization kinetics and can easily be adapted from existing jacketed agitated vessels for continuous applications.²⁷ For this reason, MSMPR crystallizers to produce active pharmaceutical ingredients (APIs) have been demonstrated in several experimental and theoretical studies. The continuous crystallization of aliskiren hemifumarate using two MSMPR crystallizers achieved both high yield and purity; growth and nucleation kinetic parameters were regressed, and yields and purities were optimized by varying MSMPR residence time and operating temperature.²⁸ The design was subsequently implemented into a CPM pilot plant.⁹ Significant

Received: July 4, 2017

Published: September 13, 2017

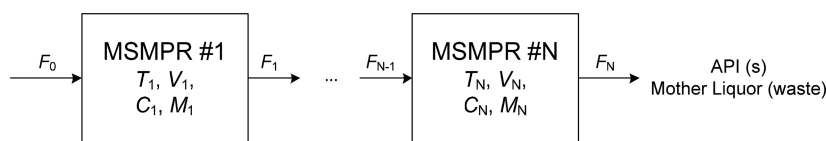


Figure 1. MSMPR crystallization of cyclosporine without process recycle.⁵³

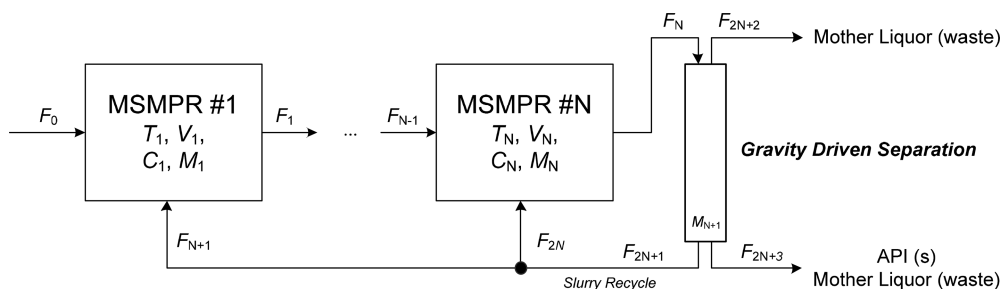


Figure 2. MSMPR crystallization of cyclosporine with solids recycle.⁵⁴

work in the MSMPR crystallization of paracetamol has been made using a series of crystallizers²⁹ with the additional consideration of filtration units,³⁰ slurry transfer^{31,32} and membrane separations^{33,34} to further develop these processes. Furthermore, various studies have used MSMPR crystallizers to control attainable crystal size distributions^{35–37} polymorphic states^{38–40} and perform enantiomeric separations^{41,42} for different products.

Experimental studies are often coupled with process modeling and simulation methodologies to construct predictive models to screen various process conditions and configurations while circumventing time and financial investments.⁴³ Computational studies for the MSMPR crystallization of various APIs are demonstrated in the literature.^{24,44–48} A recent study conducted rigorous mathematical modeling and control around a steady-state set point for the MSMPR crystallization of paracetamol, demonstrating reduced residence times and comparable yields with the batch process.⁴⁹ Another study performed kinetic parameter estimation and multiobjective optimization for the continuous crystallization of paracetamol in two MSMPRs in series.²⁹

Another API whose continuous crystallization has been demonstrated in MSMPR crystallizers is cyclosporine. Cyclosporine is an immunosuppressant drug listed on the World Health Organisation (WHO) Essential List of Medicines for the prevention of organ transplant rejection⁵⁰ with additional applications in the treatment of psoriasis, rheumatoid arthritis and dermatitis.⁵¹ The continuous cooling crystallization of cyclosporine in MSMPR crystallizers has been investigated via experimental and process modeling studies in the literature; growth and nucleation kinetic parameters have been estimated,⁵² and the viability of configurations with various recycle options^{53–55} have been considered. Process configurations with mother liquor recycle have been investigated,⁵⁵ but decreases in purity as a result of recycling made the process inferior to configurations with and without solids recycle.^{53,54} The choice of recycle option significantly affects the type and capacity of equipment required, and the selection of feasible and viable operating regimes is paramount to successful process development.^{56,57} Experimental work has yet to conduct fully rigorous, systematic comparisons of feed conditions, operating temperatures, recycle ratios and feed point locations on the performance of continuous cooling crystallization of cyclo-

sporine. A systematic technoeconomic analysis comparing different flowsheets is also yet to be conducted; costing of different configurations aids the elucidation of the best candidate process prior to scale-up.⁵⁸

This paper describes the steady-state process modeling for a systematic technoeconomic comparison of two flowsheet configurations for continuous cyclosporine crystallization in MSMPR crystallizers: the process without recycle and the process with solids recycle, based on experimentally demonstrated configurations.^{53,54} First, we describe the different flowsheets and operating variables considered in each configuration. We then describe the process modeling methodologies, combining fundamental population balance equations, crystallization kinetics and process mass balances for MSMPR crystallization. Calculated attainable crystallization and plant-wide yields and material efficiencies are compared for different configurations to establish the most promising candidate configurations for cost comparison. Subsequently, we conduct an economic analysis to compare candidate processes to evaluate the most viable configuration for application. Finally, discussion of the results and conclusions on the technoeconomic viability of different continuous processes for cyclosporine crystallization are presented with an outlook to future work in this vibrant research field.

2. PROCESS FLOWSHEETS

Here, we present flowsheet configurations and their operating variables for continuous cyclosporine crystallization. All configurations are based upon experimental demonstrations for continuous cooling crystallisation of cyclosporine from acetone.^{53,54} All plant designs are specified to produce 100 kg of cyclosporine per annum under steady-state conditions, consistent with our recent publications.^{59–63} The desired plant capacity can easily be altered in the proposed framework.

Figure 1 shows the flowsheet for the MSMPR cooling crystallization of cyclosporine without recycle based on recent experiments.⁵³ This configuration features a cascade of MSMPR crystallizers for continuous cyclosporine crystallization with magma transfer between crystallizers using peristaltic pumps.

Figure 2 shows the flowsheet for the MSMPR crystallization of cyclosporine with solids recycle.⁵⁴ A gravity-driven separation following the final crystallizer in the cascade allows

a concentrated solid slurry to be recycled back to the crystallizer cascade. We do not consider the effect of particle size distributions in this work as downstream processes such as wet-milling are not considered. The extent of solids recycle to each crystallizer is altered by varying the amount of material fed back to the process from the bottom of the gravity-driven separator. The concentration of the recycled solid slurry is controlled by the clear liquor removal ratio ($x = F_{2N+2}/F_N = 0.287$, as in the experimental demonstration⁵⁴); the removed mother liquor from the top of the column (F_{2N+2}) and that in the product magma (F_{2N+3}) are discarded as waste.

The experimental demonstrations of these process configurations separate cyclosporine via cooling crystallization, without the need for any antisolvent or source of counterions for salt formation, from a crude sample in acetone containing up to 19 different impurities.^{53,54} For this reason, the authors explicitly consider purity as an additional measure of crystallization performance. Due to the variation of sample compositions that will be present in real processes, we do not consider the effect of different process configurations on cyclosporine crystal purity in this work. It is assumed that the feed stream of cyclosporine in acetone contains negligible amounts of impurities that would affect the crystal purity attained in these processes. In real applications, consideration of crystal purity is imperative for application to meet the strict purity requirements of pharmaceutical processes.¹⁶

For both processes with and without solids recycle, we consider implementing one, two or three crystallizers in series. Total residence times of 1–15 h operation of the whole cascade are considered. For multiple MSMPRs, the operating temperature of the first crystallizer (T_1) is varied (10, 15, and 20 °C) and a final crystallizer temperature (T_N) of 0 °C is chosen, with linear temperature decrease from T_1 to T_N from the beginning to the end of the cascade. These operating variables are similar to those used in the experimental demonstrations.^{53,54}

For the process without recycle, the effect of the API feed concentration is also considered to demonstrate the sensitivity of designs to varying feed conditions; feasible feed concentrations of 20, 25 and 30% w/w are considered here. The effect of solute feed concentration on MSMPR crystallization performance has not been previously considered for continuous cyclosporine crystallization.

For the processes with solids recycle, experimental demonstrations have considered a total solids recycle extent of 90%, i.e. 90% of slurry exiting the bottom of the gravity-driven separator is fed back to the crystallization process.⁵⁴ In this work, we compare total solids recycles of 50, 70 and 90%. We also conduct a systematic comparison of varying the feed point location of the solid recycle stream via four different scenarios: the entire recycle stream fed to the first, second or third crystallizers only or the recycle stream equally distributed between all crystallizers in the cascade.

3. STEADY-STATE PROCESS MODEL AND SIMULATION METHODS

The following assumptions are involved in the formulation of the steady-state MSMPR model:⁶⁴

1. The fresh feed stream to the process is a homogeneous mother liquor containing no API crystals.
2. Crystallization birth occurs by nucleation, and crystal growth is linear. Growth is size-independent (i.e.,

McCabe's ΔL law applies), and there is no crystal breakage or attrition.

3. Product magma discharges at equilibrium from all crystallizers; i.e., the mother liquor exiting the crystallizer is saturated.
4. The contents of the crystallizer are perfectly mixed; i.e. the supersaturation field in the crystallizer is uniform, and the product magma has the same composition as the crystallizer contents.

All flowsheets and plant designs produce 100 kg of cyclosporine per annum. The steady-state process models for all flowsheet configurations describe one-dimensional crystallization kinetics, population balance equations and process mass balances. Simultaneous solution of these equations describes continuous crystallization in a series of MSMPR crystallizers.

The proposed framework models steady-state MSMPR crystallization of cyclosporine; MSMPR crystallizers are operated continuously, and thus steady-state is the dominant mode of operation during API production. The consideration of dynamic operation (e.g., for start-up procedures) requires extended modeling and solution of PDEs, which is beyond the scope of this work, but has been investigated in the literature.^{49,65}

3.1. Crystallization Kinetics. The crystallization kinetics equations describe the linear growth and nucleation rates of API crystals as a function of the supersaturation and operating temperature of the MSMPR crystallizers. The linear crystal growth rate in MSMPR i , G_i , is described by the following power law expression¹⁸

$$G_i = k_{g0} \exp\left(-\frac{E_{ag}}{R(T_i + 273.15)}\right) \left(\frac{C_i}{C_i^{\text{sat}}} - 1\right)^g \quad (1)$$

k_{g0} is the pre-exponential growth factor, E_{ag} is the growth energy barrier, R is the universal gas constant, T_i is the operating temperature of MSMPR i , C_i is the API concentration in the mother liquor within and discharged from MSMPR i and g is the crystal growth exponent. The API saturation concentration, C_i^{sat} , is a function of T_i , calculated via a surrogate polynomial regressed from published temperature-dependent saturation data for cyclosporine.⁵⁵

$$C_i^{\text{sat}} = (1.165 \cdot 10^{-4})T_i^2 + (2.000 \cdot 10^{-4})T_i + 0.047 \quad (2)$$

The nucleation rate in MSMPR i , B_i , is described by the power law expression¹⁸

$$B_i = k_{b0} \exp\left(-\frac{E_{ab}}{R(T_i + 273.15)}\right) \left(\frac{C_i}{C_i^{\text{sat}}} - 1\right)^b M_i^m \quad (3)$$

k_{b0} is the pre-exponential factor for nucleation, E_{ab} is the nucleation energy barrier, b is the crystal nucleation exponent, M_i is the slurry density in MSMPR i and m is the exponent of the slurry density. All crystallization kinetic parameters taken from previous work are listed in Table 1.⁵⁴

MSMPR crystallizers are applicable for substances with slow crystallization kinetics. The proposed framework can be implemented for any API whose crystallization kinetics are slow, for which physical properties and crystallization kinetic parameters are available and whose solubility varies significantly with temperature (i.e., API separation is amenable to cooling crystallization) can be estimated experimentally or modeled.

Table 1. Crystallization Kinetic Parameters for the Cooling Crystallization of Cyclosporine⁵⁴

parameter	value	units
k_{g0}	1.13×10^7	m min^{-1}
E_{ag}/R	9.06×10^3	K
k_{b0}	4.80×10^{20}	$\# \text{ m}^{-3} \text{ min}^{-1}$
E_{ab}/R	7.03×10^3	K
g	1.33	—
b	1.50	—
m	2/3	—

3.2. Population Balance Equations. The general one-dimensional population balance model is described by a system of ordinary differential equations (ODEs).

$$G_1 V_1 \frac{dn_1}{dL} = F_{N+1} n_{N+1} - F_1 n_1 \quad (4)$$

$$G_i V_i \frac{dn_i}{dL} = F_{i-1} n_{i-1} + F_{N+i} n_{N+i} - F_i n_i \quad i = 2 \dots N \quad (5)$$

F_{i-1} and F_i are the volumetric flow rates of streams entering and leaving MSMPR i , respectively, F_{N+i} is the recycle volumetric flow rate entering MSMPR i , N is the total number of crystallizers, n_i is the crystal population density function in MSMPR i and L is the characteristic length of the crystal. For the process without recycle, F_{N+i} terms are equal to zero. The system of ODEs formed by the population balance equations are satisfied by the boundary condition, $n_i^0 = n_i(L = 0)$, corresponding to the population density of nuclei.

$$n_i^0 = \frac{B_i}{G_i} \quad (6)$$

The slurry density in MSMPR i is calculated from the population density function as follows:⁵⁰

$$M_i = k_v \rho_{\text{API}} \int n_i L^3 dL \quad (7)$$

k_v is the crystal volume shape factor ($= \pi/6$ for spherical crystals, assumed constant for linear crystal growth) and ρ_{API} is the API crystal density. A typical value of $\rho_{\text{API}} = 1.3 \text{ g cm}^{-3}$ for solid APIs⁶⁶ is assumed here due to the lack of physical property data for cyclosporine.

3.3. Process Mass Balances. The steady-state mass balances for each process assume no material accumulation and account for volumetric changes due to API crystallization. The general mass balance equations for processes are⁵⁴

$$F_0 C_0 + F_{N+1} \left(1 - \frac{M_{N+1}}{\rho_{\text{API}}}\right) C_N + F_{N+1} M_{N+1} - F_1 \left(1 - \frac{M_1}{\rho_{\text{API}}}\right) C_1 - F_1 M_1 = 0 \quad (8)$$

$$F_{i-1} \left(1 - \frac{M_{i-1}}{\rho_{\text{API}}}\right) C_{i-1} + F_{i-1} M_{i-1} + F_{N+i} \left(1 - \frac{M_{N+1}}{\rho_{\text{API}}}\right) C_N + F_{N+i} M_{N+1} - F_i \left(1 - \frac{M_i}{\rho_{\text{API}}}\right) C_i - F_i M_i = 0 \quad i = 2 \dots N \quad (9)$$

F_0 and C_0 are the volumetric flow rate and mother liquor API concentration of the fresh feed stream, respectively. For the process without recycle, F_{N+i} terms are equal to zero.

For the solids recycle case, an additional mass balance around the gravity-driven separator is required:⁵⁴

$$M_{N+1} = \frac{M_N}{(1-x)} \quad (10)$$

where x is the clear liquor removal ratio.

For all processes, an API balance across mother liquor and crystallized solid phases also gives the following expression for the slurry density from the process mass balances:

$$M_i = C_{i-1} - C_i \quad (11)$$

3.4. Process Yields. The crystallization yield is calculated from the mother liquor API concentration exiting the final crystallizer relative to the feed concentration.

$$Y_{\text{crystallization, NR/SR}} = 100 \left(1 - \frac{C_N}{C_0}\right) \quad (12)$$

The plantwide yield is calculated from the amount of crystallized API in the product magma stream relative to the total mass of API in the fresh process mother liquor feed stream. For the process without recycle the crystallization and plantwide yields are equal; i.e., the product stream is that leaving the final crystallizer (F_N in Figure 1) and the product stream is the concentrated magma leaving the bottom of the gravity-driven separator withdrawn as product (not recycled, F_{2N+3} in Figure 2). For the process with solids recycle, the plantwide yield is calculated from the mass of crystallized API withdrawn from the bottom of the gravity-driven separator as product (F_{2N+3} in Figure 2) relative to the amount in the feed mother liquor to the process (F_0).

$$Y_{\text{plantwide, NR}} = Y_{\text{crystallization, NR}} \quad (13)$$

$$Y_{\text{plantwide, SR}} = 100 \left(\frac{F_{2N+3} M_{N+1}}{F_0 C_0}\right) \quad (14)$$

3.5. Environmental Impact Assessment. A measure of the environmental impact of different processes is essential in addition to the calculation of attainable crystallization and plantwide yields. Measuring the material efficiency of a process provides an indication of the amount of waste that will be produced, which in turn is a measure of the environmental impact of the process. Green chemistry metrics allow the quantitative comparison of the material efficiencies of different processes.⁶⁷ The choice of an appropriate green chemistry metric depends upon the studied process.⁶⁸ The environmental (E)-factor is a commonly used, flexible green chemistry metric that quantifies the mass of waste produced per unit mass of desired product.

$$E = \frac{m_{\text{waste}}}{m_{\text{API}}} \quad (15)$$

We quantify the material efficiencies of different flowsheet configurations via the E -factor in this work. For all configurations, waste components are considered as the unrecovered mother liquor streams. The process without recycle has unrecovered mother liquor leaving in the product magma from the final crystallizer (F_N in Figure 1); the process with solids recycle has mother liquor removed from the top and

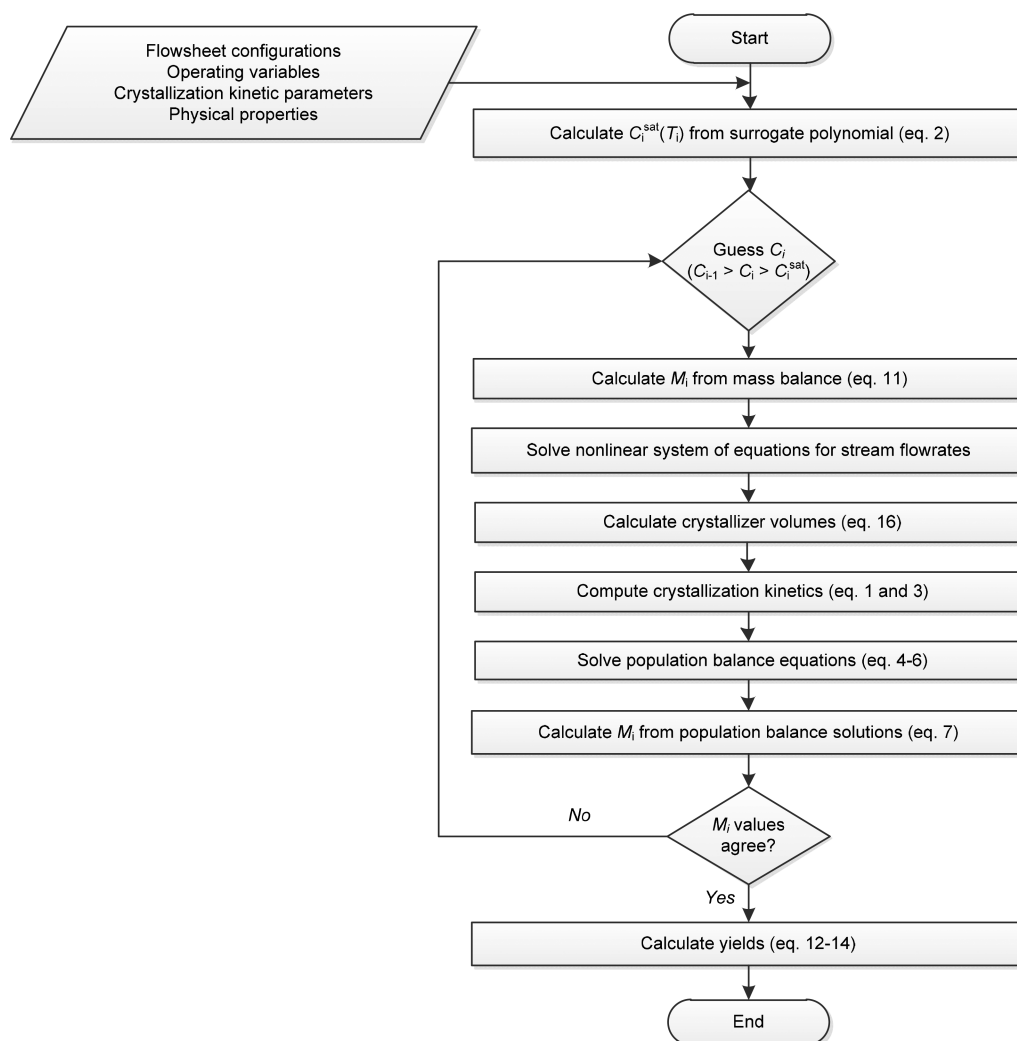


Figure 3. Algorithm flowchart for the solution of the steady-state process model for continuous cyclosporine crystallization in MSMMPR crystallizers.

bottom of the column (F_{2N+2} and F_{2N+3} in Figure 2, respectively).

3.6. Calculation of Crystallizer Volumes. The calculation of required crystallizer volumes is required for solutions of the population balance equations in the steady-state process model and for cost calculations. Required crystallizer volumes are calculated from the total residence time of the MSMMPR cascade and the process volumetric flow rates of the process. For N crystallizers in series, the residence time of each crystallizer is the total cascade residence time divided by N ; thus, the required crystallizer volume is calculated as

$$V_N = F_i \tau_i = \frac{F_i \tau_{\text{total}}}{N} \quad (16)$$

The model considers the residence times of the main process stream in the MSMMPR crystallizers only. The residence times of streams in the solids recycle loop are not considered here due to the small API capacity and crystallizer volumes. The effect of recycle stream residence times will become more significant for increased plant capacities and should be considered in scale-up studies. For subsequent economic analyses, volumetric flow rates and crystallizer volumes are scaled to account for crystallization and plantwide inefficiencies.

3.7. Algorithm and Code Structure. Figure 3 shows the algorithm flowchart for the solution of different process

configurations for continuous cyclosporine crystallization in MSMMPR crystallizers. An initial guess must be made for the vector of outlet concentrations of each MSMMPR crystallizer (C_i), which must lie between the crystallizer inlet concentration (C_{i-1}) and the saturation concentration at T_i (C_i^{sat}); this guess is close to the saturation concentration for each crystallizer, which allowed convergence when validating the model versus experimental results.^{53,54,69} The slurry densities in each crystallizer (M_i) are computed, which are used to solve mass balances for the process' volumetric flow rates. Required crystallizer volumes are calculated from the total cascade residence time and the calculated volumetric flow rates. Crystallization kinetics, stream flow rates and crystallizer volumes are then incorporated into the population balance equations. The population balance equations are then solved, and the slurry densities are calculated. The difference between the slurry densities calculated from the mass balance equations and the population balance solutions form a system of nonlinear equations that is solved by iterating upon the vector of C_i values.

The process model is implemented and solved in MATLAB. The population balance equations form a system of stiff ODEs which are solved using the built-in solver ode15s. The system of nonlinear equations formed by the differences between slurry densities calculated from mass balances and population balance

Table 2. Equipment Parameters for Calculating Scaled Equipment Purchase Costs in the Present Day

item	ref. year	ref. cost, P_A (GBP)	capacity basis	ref. capacity, S_A	n	f (%)	ref.
crystallizer	2007	328 875	m ³	3.00	0.53	10.33	70
pump	2015	958	—	—	1.00	—	71
gravity-driven separator	2007	207 900	L s ⁻¹	58	0.64	10.33	70

equations is solved using the built-in solver *fsolve* (with tolerances of 10^{-6}). A variety of initial guesses for C_i gave the same converged results for all values used. The process model has been validated by replicating process yields for various experimental studies.^{53,54,69}

4. ECONOMIC ANALYSES

Systematic cost analyses are essential to inform the selection of economically viable process options. Our recent work^{59–63} has utilized an established methodology for costing batch and CPM processes.⁵⁸ The studied processes are assumed to be implemented at an existing pharmaceutical manufacturing site with essential auxiliary structures already in place. 8000 h of operation per year is considered. Here, we describe the costing methodology used in this work.

4.1. Capital Expenditure (CapEx). Prices for equipment of similar capacities to those considered here have been sourced where possible; when such data are unavailable, the following cost–capacity correlation is used:⁷⁰

$$P_B = fP_A \left(\frac{S_B}{S_A} \right)^n \quad (17)$$

P_i is the equipment purchase cost at capacity S_i . The exponent n depends on the equipment item. Varying design considerations between different equipment capacities are accounted for via the factor f . Values of n and f are found in the literature.⁷⁰ Where the reference purchase costs (P_A) are taken from the past, chemical engineering plant cost indices (CEPCIs) are used to account for inflation. All equipment capacities are scaled to account for plantwide inefficiencies to meet the specified plant capacity. MSMPR crystallizers are modeled as forced circulation crystallizers, peristaltic pumps are used for feed transfer, recycle and product streams,^{53,54} and the gravity-driven separator is modeled as a solid settler. Table 2 gives details for the purchase costs and scaling parameters in eq 17 for each equipment item used in processes with and without solids recycle.

The sum of all inflation-adjusted equipment purchase costs gives the Free-on-Board (FOB) cost. The Chilton method is used to calculate the Battery Limits Installed Cost (BLIC).⁷² The installed equipment cost (IEC) is calculated as 1.43 times the FOB. Process piping and instrumentation (PPI) costs are calculated as 42% of IEC, respectively. The sum of IEC and PPI gives the total physical plant cost (TPPC). A construction factor of 0.3 is added to TPPC to calculate the BLIC.⁵⁸

$$\text{IEC} = 1.43\text{FOB} \quad (18)$$

$$\text{PPI} = 0.42\text{IEC} \quad (19)$$

$$\text{TPPC} = \text{IEC} + \text{PPI} \quad (20)$$

$$\text{BLIC} = 1.3\text{TPPC} \quad (21)$$

Working capital costs are taken as 3.5% of annual material costs ($\text{MAT}_{\text{annual}}$).⁵⁸ Contingency costs (CC) are calculated as 20% of the BLIC. The sum of working capital and contingency

costs (WCC) and BLIC gives the total capital expenditure (CapEx) of the process.⁵⁸

$$\text{WC} = 0.035\text{MAT}_{\text{annual}} \quad (22)$$

$$\text{CC} = 0.2\text{BLIC} \quad (23)$$

$$\text{WCC} = \text{WC} + \text{CC} \quad (24)$$

$$\text{CapEx} = \text{BLIC} + \text{WCC} \quad (25)$$

4.2. Operating Expenditure (OpEx). Annual operating expenditure ($\text{OpEx}_{\text{annual}}$) is calculated as the sum of annual material ($\text{MAT}_{\text{annual}}$), utilities and waste disposal ($\text{UW}_{\text{annual}}$) costs. Material purchase prices are sourced from various vendors. All material requirements are scaled to account for plantwide inefficiencies to meet the specified plant capacity (100 kg per annum). Annual utilities costs ($\text{UTIL}_{\text{annual}}$) are calculated as 0.96 GBP per kg of material input (total feed mother liquor);⁵⁸ a coefficient of 460.8 is used to convert the mass flow rate to kg y⁻¹ for economic analysis calculations. Annual waste costs ($\text{Waste}_{\text{annual}}$) are 0.35 GBP per L of waste produced;⁵⁸ a coefficient of 168 is used to convert the volumetric flow rate to L y⁻¹.

$$\text{UTIL}_{\text{annual}} = 460.8F_0(\rho_{\text{acetone}} + C_0) \quad (26)$$

$$\text{Waste}_{\text{annual}} = 168 \frac{F_N}{\rho_{\text{acetone}}} \left[\left(1 - \frac{M_N}{\rho_{\text{API}}} \right) C_N + \rho_{\text{acetone}} \right] \quad (27)$$

$$\text{UW}_{\text{annual}} = \text{UTIL}_{\text{annual}} + \text{Waste}_{\text{annual}} \quad (28)$$

$$\text{OpEx}_{\text{annual}} = \text{MAT}_{\text{annual}} + \text{UW}_{\text{annual}} \quad (29)$$

We consider all mother liquor unrecovered for all process configurations. Labour costs are not considered here due to the small scale of production and automated nature of CPM.

4.3. Total Costs. The total cost of the plant designs is calculated as the sum of CapEx and inflation-adjusted OpEx over the plant lifetime.

$$\text{Total Costs} = \text{CapEx} + \sum_{k=1}^{\tau} \frac{\text{OpEx}_{\text{annual}}}{(1+r)^k} \quad (30)$$

where CapEx is the sum of BLIC and WCC (eq 25) and $\text{OpEx}_{\text{annual}}$ is the sum of $\text{MAT}_{\text{annual}}$ and $\text{UW}_{\text{annual}}$ adjusted for inflation over the total plant lifetime. Total material and utilities and waste disposal costs (the sum of which give the total OpEx, $\text{OpEx}_{\text{total}}$) are calculated and adjusted for inflation over the total plant lifetime.

$$\text{MAT}_{\text{total}} = \sum_{k=1}^{\tau} \frac{\text{MAT}_{\text{annual}}}{(1+r)^k} \quad (31)$$

$$\text{UW}_{\text{total}} = \sum_{k=1}^{\tau} \frac{\text{UW}_{\text{annual}}}{(1+r)^k} \quad (32)$$

$$\text{OpEx}_{\text{total}} = \text{MAT}_{\text{total}} + \text{UW}_{\text{total}} \quad (33)$$

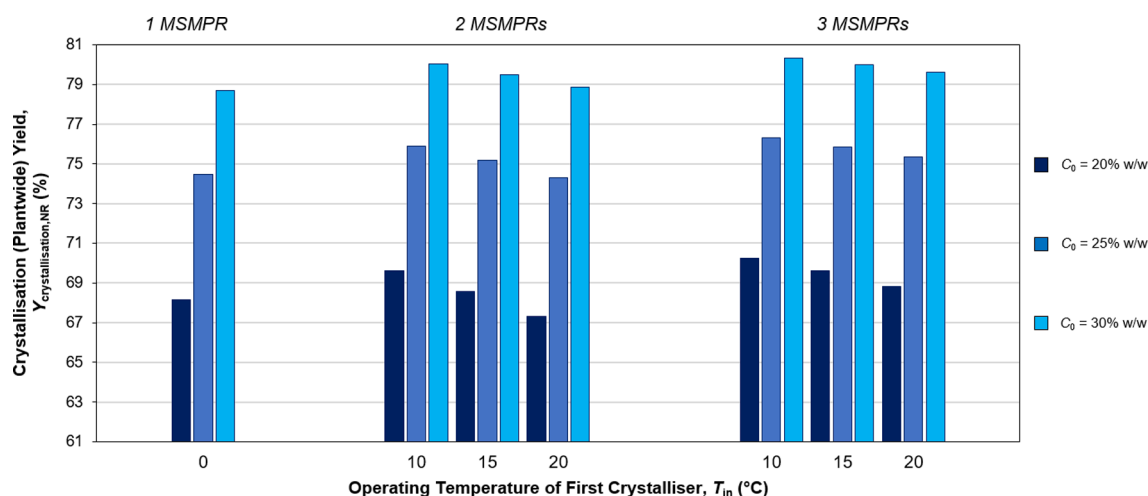


Figure 4. Attainable crystallization (plantwide) yields, $Y_{\text{crystallization,NR}} = \left(1 - \frac{C_N}{C_0}\right) \cdot 100\%$, for continuous cyclosporine crystallization without recycle (total cascade residence time = 12 h).

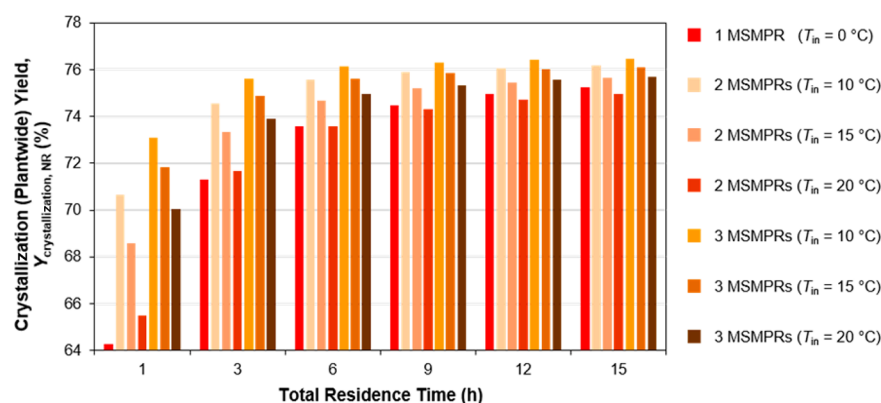


Figure 5. Attainable crystallization (plantwide) yields, $Y_{\text{crystallization,NR}} = \left(1 - \frac{C_N}{C_0}\right) \cdot 100\%$, for continuous cyclosporine crystallization without recycle as a function of total residence time ($C_0 = 25\%$ w/w).

A plant-operating lifetime (τ) of 20 years and an interest rate (r , accounting for inflation) of 5% are considered. All CapEx is assumed to occur in year 0, and operation is assumed to begin in year 1.

The most economically viable process is that which ultimately achieves the lowest total costs and environmental impact (i.e., E -factors) over the specified plant lifetime. Total costs (CapEx and OpEx components) are systematically compared for each entire process configuration.

5. RESULTS AND DISCUSSION

5.1. Attainable Yields and Material Efficiencies.

5.1.1. No Recycle. The effect of API feed concentration was considered for the continuous cyclosporine crystallization without recycle. Figure 4 shows the attainable yields for a varying number of crystallizers and total MSMPR cascade residence time of 12 h. The results show that the considered API feed concentration has a significant impact on the attained yield; this is an important variable due to potential fluctuations in feed composition to a continuous crystallization process. Consideration of unit operations required to meet the specified feed concentration for a designed crystallization process is paramount to successful operation, and should be considered

for further investigations encompassing upstream unit operations prior to crystallization.

The results also show that increasing the number of crystallizers and decreasing the operating temperature leads to an increase in crystallization yield. Reducing the operating temperature increases the supersaturation, which enhances the yield. Increasing the number of crystallizers over which cooling to the target temperature is attained also enhances the yield as well as reducing the specific cooling duty per crystallizer.⁶⁴

The effect of varying the total cascade residence time for the process without recycle was then investigated. Figure 5 shows the attainable yields as a function of the number of crystallizers, the operating temperature and the total cascade residence time for a feasible API feed concentration of 25% w/w. The results show flattening profiles for all process configurations beyond a total cascade residence time of 9 h, from which there are only incremental increases in attainable yield. It is also observed that using three crystallizers and operating the first crystallizer at 10 °C gives the highest attainable yields for any total residence time considered. These results show that using multiple crystallizers allows higher attainable yields than a single crystallizer for the same total residence time for certain operating temperatures.

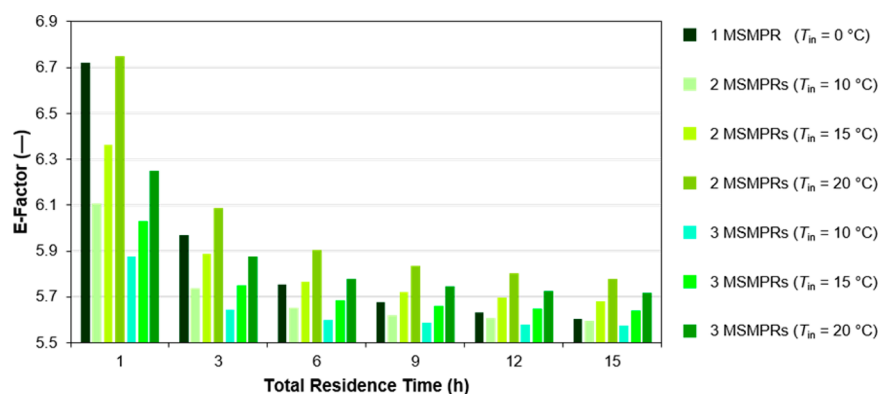


Figure 6. *E*-factors for continuous cyclosporine crystallization without recycle.

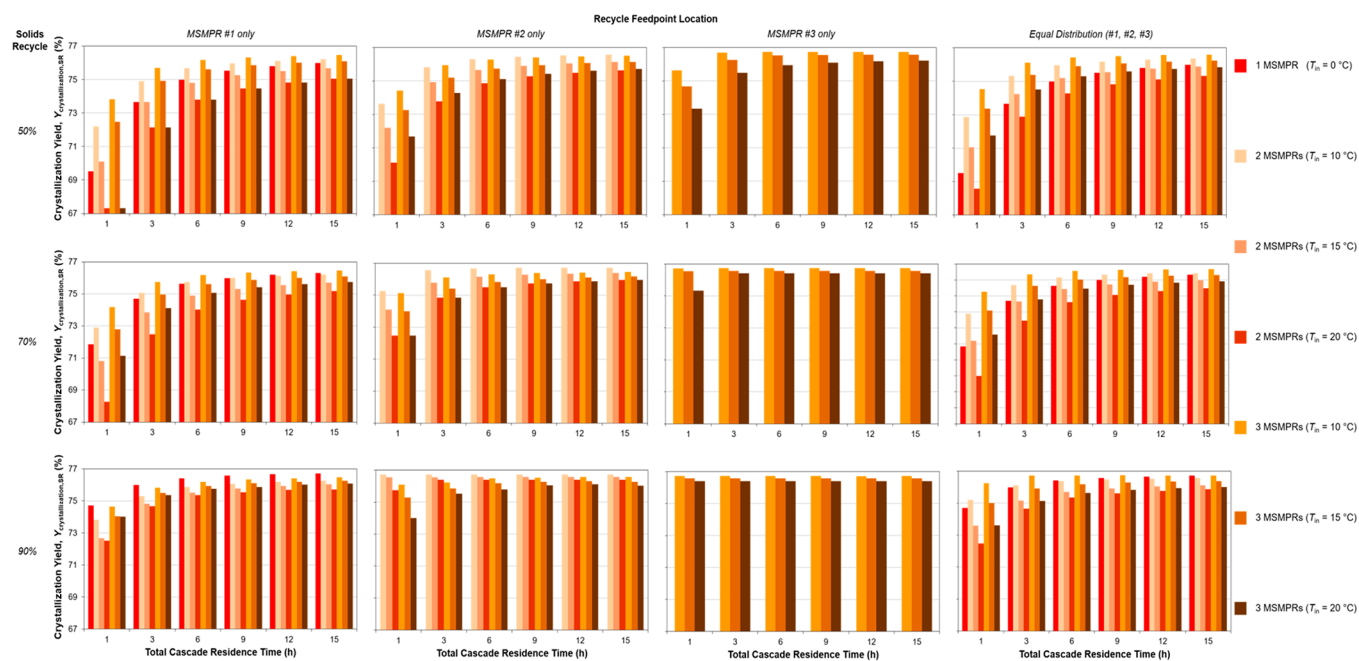


Figure 7. Attainable crystallization yields, $Y_{\text{crystallization,SR}} = \left(1 - \frac{C_N}{C_0}\right) \cdot 100\%$, for continuous cyclosporine crystallization with solids recycle as a function of total residence time ($C_0 = 25$ w/w %).

Figure 6 shows the *E*-factors for the process without recycle corresponding to the attainable yields presented in Figure 5. The process configuration with no recycle achieves very low *E*-factors due to the high yields and simplicity of the process in comparison with other purification and separation technologies, e.g. liquid–liquid extraction or antisolvent crystallization that require an additional solvent to induce phase separation. The *E*-factor can be as high as 200 for batch-dominated processes such as those implemented in the pharmaceutical industry, whereas continuously operated manufacturing methods such as petroleum-based processes can have *E*-factors as low as 0.1.⁷³ Pharmaceutical processes also have typically high *E*-factors due to the inherent complexity of their processes involving multistep syntheses, intermediate workups and purifications and downstream operations required to meet the strict product standards for pharmaceutical products.

5.1.2. Solids Recycle. Figure 7 shows the calculated attainable crystallization yields for the process with solids recycle (i.e., the amount of API crystallized from mother liquor in the stream exiting the final crystallizer, F_N) for an API feed

concentration of 25% w/w. Crystallization yields improve with increasing recycle ratio due to the enhanced crystal surface area in the crystallizer.⁵⁴ The effect of the recycle feed point location has also been investigated. It is shown that feeding the solids recycle stream to the final crystallizer provides the greatest yields for all operating temperatures and residence times considered. The effect of these different extents of recycle and feed point location directly affects the required crystallizer volumes, which will impact the CapEx of the process; economic analyses can further elucidate the most viable process configuration. It is also shown in Figure 7 that certain recycle ratios (e.g., 90%) attain higher crystallization yields when using a single crystallizer instead of multiple units. This result highlights the need for systematic screening of different process options to establish viable configurations.

Figure 8 shows the plantwide yields (i.e., the amount of solid API removed as product from the bottom of the gravity-driven separator in stream F_{2N+3}) following gravity-driven separation for the process with solids recycle. In contrast to the results for crystallization yields (Figure 7), increasing the recycle ratio

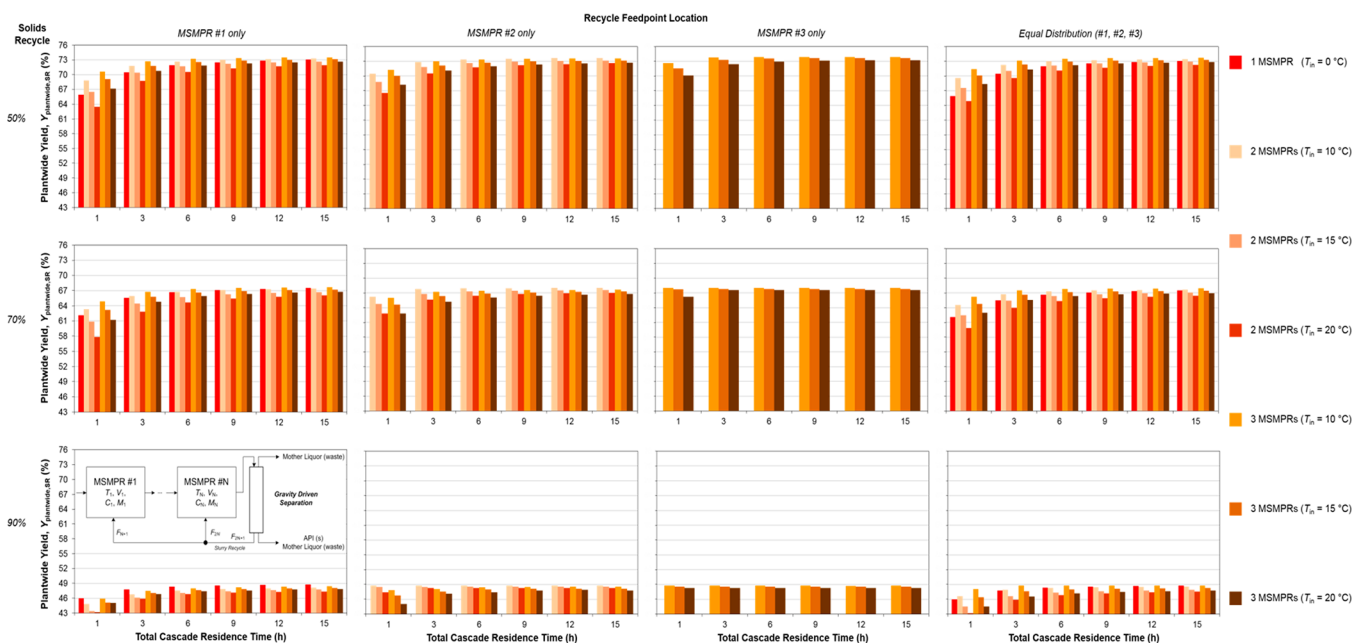


Figure 8. Attainable plantwide yields, $Y_{\text{plantwide,SR}} = \left(\frac{F_{2N+3}M_{N+1}}{F_0C_0} \right) \cdot 100\%$, for the continuous crystallization of cyclosporine with solids recycle as a function of total cascade residence time ($C_0 = 25$ w/w %).

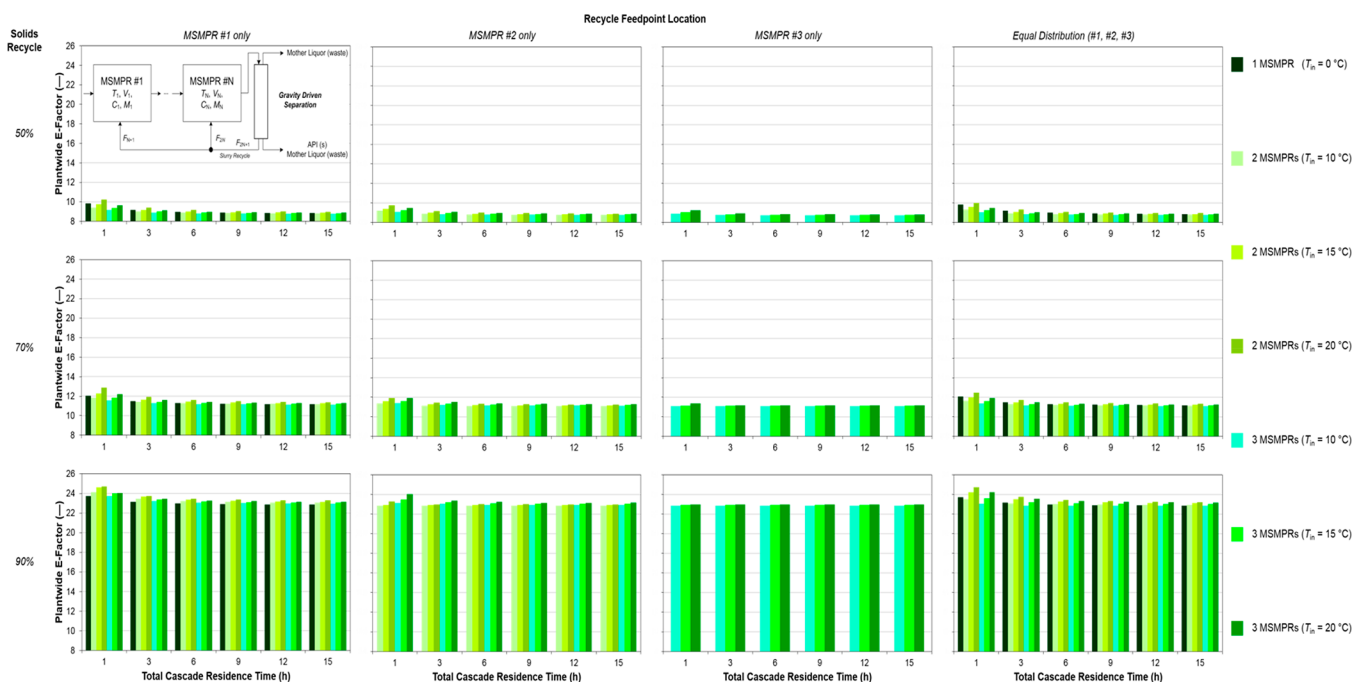


Figure 9. Plantwide E -factors for the continuous cyclosporine crystallization with solids recycle as a function of total cascade residence time ($C_0 = 25$ w/w %).

leads to a decrease in plantwide yield. This is due to the increased amount of mother liquor containing uncrystallized API which is discharged from the top and bottom of the gravity-driven separator with increasing recycle ratios. This also incurs a decreased plant productivity due to the increasing amount of solids fed back to the crystallizer cascade as opposed to being withdrawn as product. This effect is a result of the flowsheet configuration we have modeled here, based upon the demonstrated experimental setup.⁴⁵ This is an important implication when considering the design and implementation

of continuous crystallization processes. The loss of API in mother liquor streams can be controlled by altering the clear mother liquor removal ratio (x), but this will also affect the attainable crystallization yield. Further investigation via a wider multivariate analysis of the process with solids recycle is required to identify the best configuration for this process.

Figure 9 shows the E -factors corresponding to the plantwide yields for the process with solids recycle. The waste streams of the process with solids recycle are the mother liquor streams removed from the top and bottom of the gravity-driven

separator. For increased recycle ratios, the E -factors of different process options increase due to the decreasing plantwide yields with increasing recycle ratio. This is due to the increased amount of mother liquor which is discharged from the process as waste with increasing recycle ratio, as well as the increased material requirements needed to account for plantwide inefficiencies to meet the specified plant capacity. Despite the elevated E -factors for higher recycle ratios, the values for all processes considered are acceptable for pharmaceutical processes.⁷³

5.2. Crystallizer Volume Design. From the calculated attainable crystallization and plantwide yields presented, it is shown that beyond certain residence times, there is no appreciable increase in yield. Designing cascades with longer residence times (i.e., crystallizers with working volumes significantly larger than necessary) will result in economically unviable process designs. The effect of different process configurations impacts the total crystallizer volumes required which directly affects the capital costs of the design. We calculate crystallizer volumes as a function of operating temperature, the number of crystallizers and the extent and feed point location of solids recycle. Maximum residence times beyond which there is no appreciable increase in yield (considered to be <1% relative increase in yield) were selected for economic analyses of different process options, which are shown in Table 3.

5.2.1. No Recycle. Required crystallizer volumes for the process without recycle are shown in Figure 10. Increasing the number of crystallizers allows significantly lower total crystallizer volumes due to the higher yields attainable at shorter residence times. When multiple crystallizers are used, the operating temperature has only a small effect on the total crystallizer volume due to its small effect on the process yields. When three crystallizers are used, operating the first crystallizer at 20 °C leads to a significant increase in total crystallizer volume (compared to operating at 10 and 15 °C) due to the longer residence time, and thus total crystallizer volume, required to reach the maximum attainable yield.

5.2.2. Solids Recycle. Required crystallizer volumes for the process with solids recycle are shown in Figure 11, corresponding to the maximum residence times listed in Table 3. Similar effects of increasing the number of crystallizers and varying operating temperatures are observed as for the process without recycle.

Increasing the extent of recycle leads to larger crystallizer volumes as the internal flow rates of the system become larger. The effect of feed point location on crystallizer volumes is also important; when the recycle stream is fed to the first crystallizer, all crystallizers have similar volumes as a large volumetric flow rate passes through all. A similar effect is observed when the recycle stream is equally distributed between all crystallizers. However, when the recycle stream is fed to the second or third crystallizers, only these crystallizers must be larger to accommodate the higher throughput.

5.3. Economic Analyses. In this section, we present the results of the economic analyses of different process options for the established maximum residence times listed in Table 3. Crystallizer purchase costs are a significant portion of BLIC, and thus the CapEx, so correlating crystallizer volumes with process costs provide insight into differences in total costs between different process configurations. We then present total cost components for all configurations computed using the established costing methodology described previously.⁵⁸

Table 3. Total Cascade Residence Times (h) Used for Economic Analyses, Corresponding to Maximum Yields

		no recycle			
		T_1 (°C)			
no. MSMPRs	recycle feed point	0	10	15	20
1	n/a	9	–	–	–
2	n/a	–	6	6	6
3	n/a	–	3	3	6
		solids recycle = 50%			
		T_1 (°C)			
no. MSMPRs	recycle feed point	0	10	15	20
1	MSMPR 1	6	–	–	–
	MSMPR 1	–	6	6	6
2	MSMPR 2	–	3	3	6
	equal distribution	–	3	6	6
3	MSMPR 1	–	3	3	6
	MSMPR 2	–	3	3	6
	MSMPR 3	–	3	3	3
	equal distribution	–	3	3	6
		solids recycle = 70%			
		T_1 (°C)			
no. MSMPRs	recycle feed point	0	10	15	20
1	MSMPR 1	6	–	–	–
	MSMPR 1	–	3	6	6
2	MSMPR 2	–	3	3	3
	equal distribution	–	3	6	6
3	MSMPR 1	–	3	3	6
	MSMPR 2	–	3	3	3
	MSMPR 3	–	1	1	3
	equal distribution	–	3	6	3
		solids recycle = 90%			
		T_1 (°C)			
no. MSMPRs	recycle feed point	0	10	15	20
1	MSMPR 1	3	–	–	–
	MSMPR 1	–	3	3	3
2	MSMPR 2	–	1	1	1
	equal distribution	–	3	3	3
3	MSMPR 1	–	3	3	3
	MSMPR 2	–	1	1	3
	MSMPR 3	–	1	1	1
	equal distribution	–	1	3	3

5.3.1. No Recycle. Figure 12 shows the total costs and the contributing components of different configurations for the process without recycle. In all scenarios, the BLIC contributes the most significant portion of CapEx; WCC provides a lesser contribution to CapEx due to the automated nature of continuous manufacturing processes. The process using a single crystallizer operating at 0 °C has the lowest total costs due to the significantly reduced CapEx (BLIC and WCC) costs. This result shows that increasing the number of crystallizers, and thus the number of associated pumps, has a significant impact on the total costs of the plant at this operating scale.

The most significant contribution toward OpEx is utilities and waste handling (UW). Material costs for this process are relatively small due to the nature of the crystallization process; i.e., we only consider cooling crystallization of an API from mother liquor. Material costs for more elaborate processes (e.g., encompassing syntheses, workups and purifications prior to crystallization) are much more significant in comparison to the

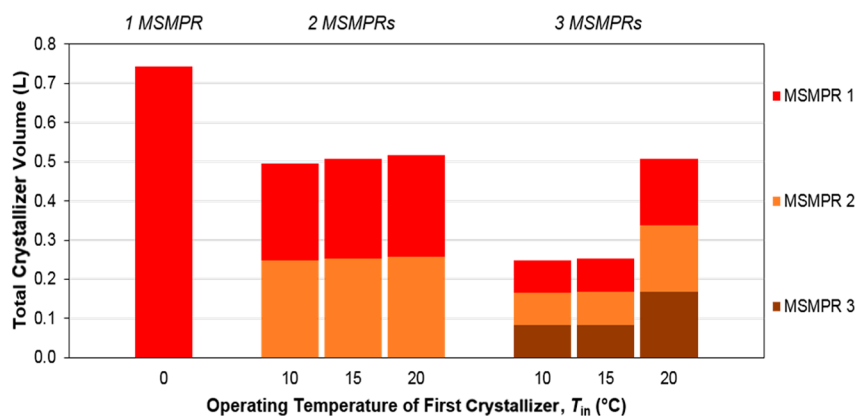


Figure 10. Calculated crystallizer volumes for residence times provided in Table 3 for the process without recycle ($C_0 = 25\%$ w/w).

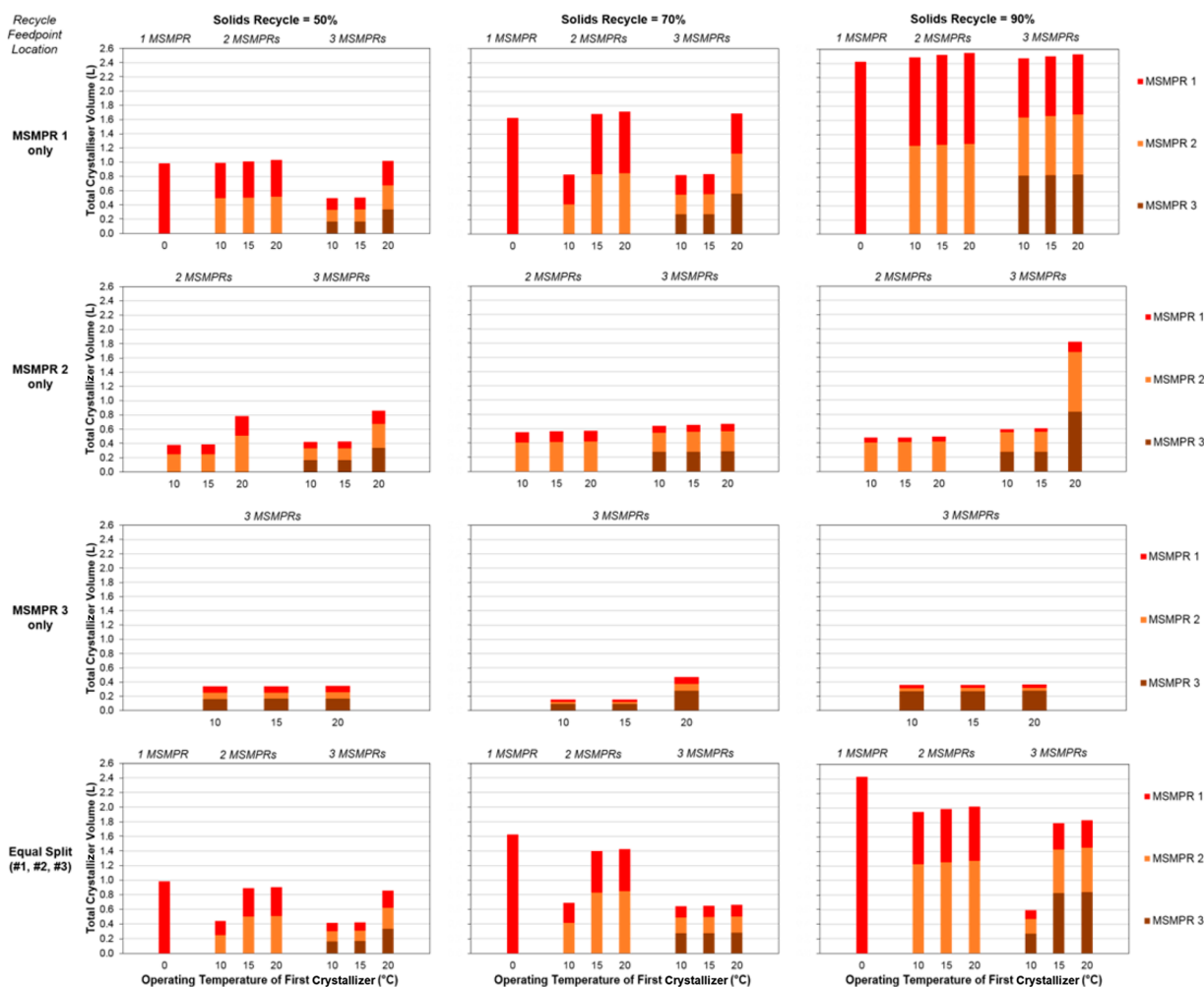


Figure 11. Calculated crystallizer volumes for residence times provided in Table 3 for the process with solids recycle ($C_0 = 25\%$ w/w).

continuous cooling crystallization process considered here. It is also observed that OpEx components (materials, utilities and waste) are relatively consistent across all scenarios for the process with no recycle; this is due to the material requirements and waste quantities being relatively similar across all processes, despite the varying number of crystallizers and operating temperatures. Explicit consideration of the effect of varying operating temperatures and pumping duties on the utilities costs is not considered in the methodology used here. This will likely lead to greater OpEx costs when operating a single

crystallizer at 0 °C as the cooling duty is burdened on one vessel only. Methodologies which explicitly calculate varying costs of utilities with differing pumping requirements and cooling duties should be implemented where possible.

5.3.2. Solids Recycle. Figure 13 shows the cost components of different configurations for the process with solids recycle. The most cost optimal configuration is using two crystallizers with all recycle fed to the first crystallizer, operating at 10 °C. As before, increasing the number of crystallizers significantly increases the CapEx of the process.

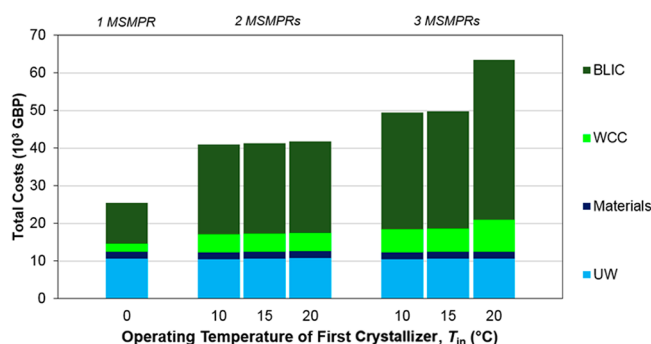


Figure 12. Cost components for the continuous cyclosporine crystallization without recycle ($C_0 = 25\%$ w/w).

Increasing the extent of solids recycle and feeding the recycle to the first crystallizer leads to increased total costs due to the increased crystallizer volumes required to handle higher material throughputs. The greatest costs incurred are when the recycle stream is evenly split between all crystallizers due to the large vessel volumes required to accommodate the increased internal flow rates and the lower yields attained in comparison to when the recycle stream is fed to the final

crystallizer. As before, BLIC contributes a significant portion to CapEx and UW contributes a significant portion to OpEx. The increased utilities costs with increasing recycle ratios, i.e. additional pumping requirements, are not explicitly considered here, but will lead to increased OpEx for scenarios with higher recycle ratios. Consideration of these factors is essential for accurate cost comparisons.

5.3.3. Cost Components per Total Crystallizer Unit Volume. In the previous subsection, Figures 12 and 13 compare absolute total cost components for all process configurations considered for the total cascade residence times listed in Table 3. As explained previously, the selection of these total cascade residence times is such that the designed crystallizers are not oversized; i.e., no unnecessary additional capital costs for crystallizers are incurred for only incremental increases in yield. However, this can lead to unfair cost comparisons due to the differences in total cascade residence times, and thus different crystallizer volumes, which significantly affects CapEx. We have calculated the total cost components normalized with respect to the total crystallizer volume in MSMPR cascades for both processes with and without solids recycle to allow an alternative economic comparison of different configurations.

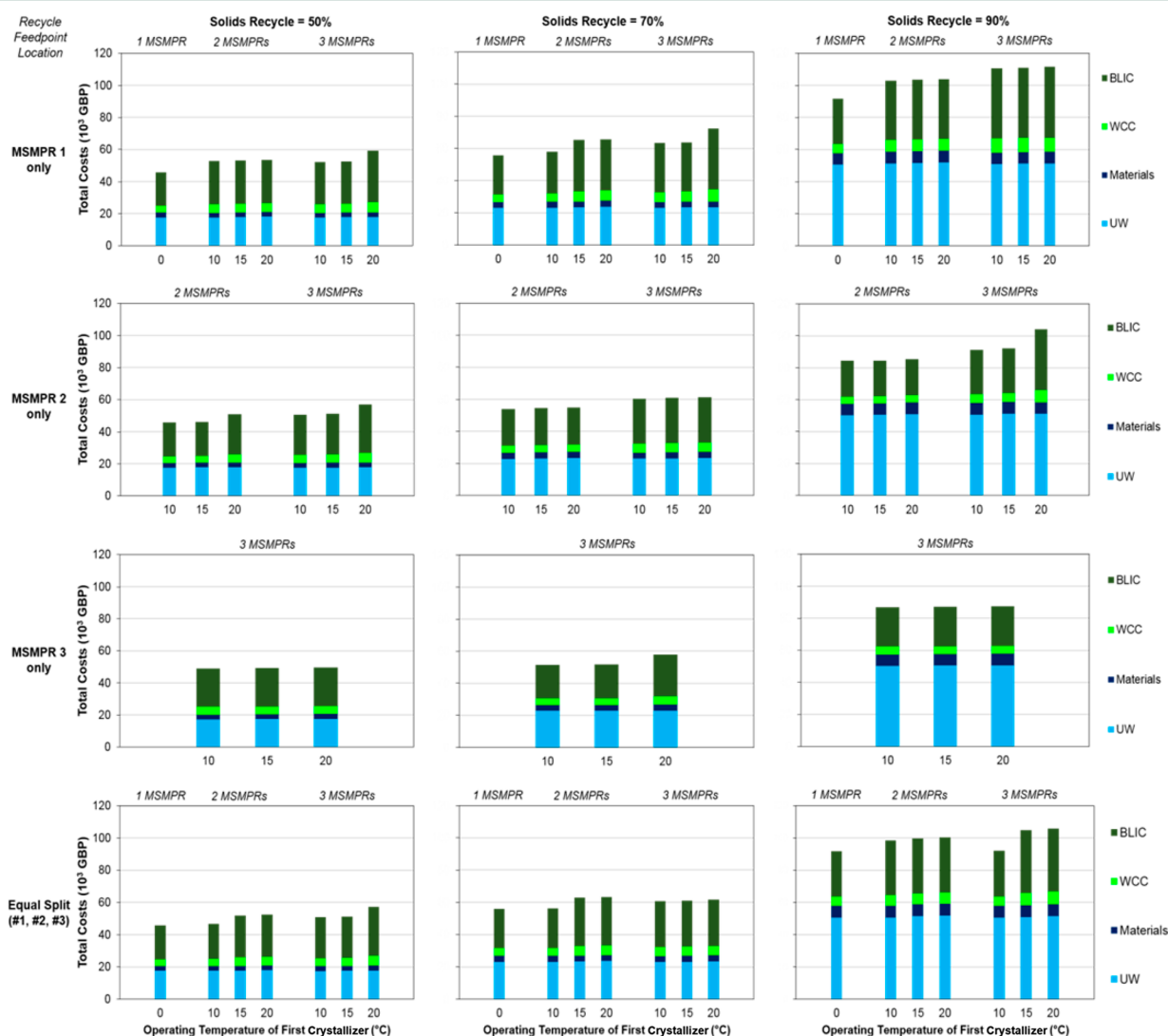


Figure 13. Cost components for the continuous cyclosporine crystallization with solids recycle ($C_0 = 25\%$ w/w).

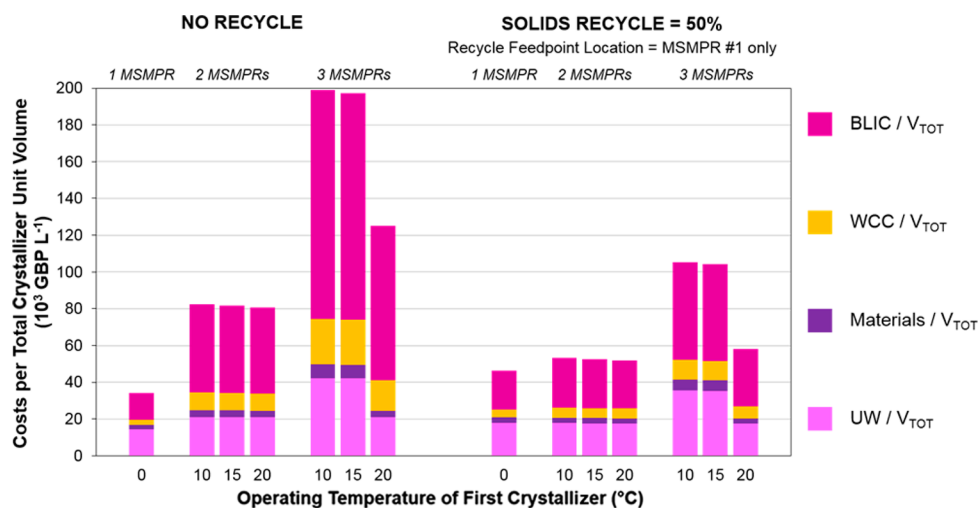


Figure 14. Cost components per total crystallizer unit volume for continuous cyclosporine crystallization without recycle (left) and with 50% solids recycle fed to the first crystallizer only (right).

Figure 14 shows normalized cost components for the process with no recycle, and the process with 50% solids recycle fed to the first crystallizer only. When one crystallizer is implemented, the normalized total costs are greater when solids recycle is implemented, due to the increased crystallizer volume required to handle recycle flow rates, which incurs greater CapEx. However, when two or three crystallizers are implemented, the process with solids recycle has lower normalized cost components. It is also shown that for both processes with and without recycle, there is a large difference between operating the first crystallizer at 15 and 20 °C when three crystallizers are implemented; this is due to the sharp increase in total crystallizer volumes for both cases.

These results indicate that the cost components of the process are sensitive to the selection of total cascade residence time for crystallization process design; i.e., if different residence times were selected for the process with solids recycle, then it should be more economically viable than the process with no recycle. This demonstrates the importance of rigorous process analysis and fair comparisons of design and operating variables for economic analyses of candidate configurations.

6. DISCUSSION

Continuous crystallization using a cascade of MSMPR crystallizers has been systematically compared via steady-state process modeling, comparing computed attainable yields, material efficiencies and total cost components. The aim of this work was to allow rigorous evaluation of economically viable options for continuous cyclosporine crystallization.

Continuous cyclosporine crystallizations for different process configurations (with and without solids recycle) have been compared as a function of the number of implemented crystallizers, total cascade residence times, operating temperatures, varying extents of solid recycle and different recycle feed point locations. Crystallization and plantwide yields, *E*-factors, required crystallizer volumes and total cost components are compared for different process configurations to evaluate the most economically viable process option. We have also calculated total cost components normalized with respect to the total crystallizer volume to highlight the sensitivity of the designs to the total cascade residence time for economic analyses.

Crystallization yields are shown to increase for greater total residence time and number of crystallizers, lower operating temperatures and higher recycle ratios. However, increased recycle ratios incur lower plantwide yields and higher *E*-factors due to greater losses of API and solvent in discharged mother liquor streams. This effect is a consequence of the equipment arrangement in the flowsheet based upon an experimental demonstration.⁴⁵ Future work should compare alternative arrangements for solids recycle to mitigate losses with increased solids recycle.

The most economically viable configuration for the process without recycle implements a single crystallizer operating at 0 °C, incurring total costs of 25 488 GBP. For the process with solids recycle, the most economically viable process option implements two crystallizers with 50% solids recycle fed to the second crystallizer only, operating the first crystallizer at 10 °C, incurring total costs of 45 660 GBP. However, as shown from the normalized cost components with respect to total crystallizer volume, these cost estimates are very sensitive to the total cascade residence time of different configurations. Future work should consider a more systematic methodology for economic analyses. The CapEx incurred when implementing multiple crystallizers and the gravity-driven separation column, for the process with solids recycle, leads to high total costs. Utilities and waste handling costs contributing to OpEx for other configurations lead to economically inferior processes compared to the process without recycle. However, the economic analysis methodology implemented here does not explicitly consider the effect of different operating temperatures and extents of recycle (which directly impact cooling and pumping duties of crystallizers and peristaltic pumps, respectively) on OpEx contributions to total costs. This may lead to reduced cost benefits when implementing a single crystallizer with a high cooling duty in comparison to other configurations which distribute the total cooling duty among multiple vessels. Future work should consider these factors for a more accurate evaluation of economically viable processes.

The steady-state process modeling results presented here are based upon several key assumptions of the MSMPR model. Neglecting the presence of impurities in the process feed stream is an important assumption; crystal purity is an essential parameter due to the strict regulations imposed on

pharmaceutical products. Moreover, the results are also strongly dependent on the limited set of operating variables (i.e., the number of crystallizers in series, total cascade residence time, operating temperature, extent and location of solids recycle). While the set and range of operating variables considered here are limited, we have chosen these ranges in accordance with those investigated in the experimental demonstrations of continuous cyclosporine crystallization.^{52–54} The process model has been described in enough detail such that the effect of operating variables beyond the sets considered here can be considered by an expert reader.

This work considers the steady-state process modeling and simulation for continuous cyclosporine crystallization and does not consider upstream synthetic steps. The continuous flow synthesis or cyclosporine is not modeled in this work due to the lack of experimental demonstrations and kinetic data required for accurate reactor design. However, the results presented here provide a direct indication of which crystallization processes will lead to the best-performing process configurations.

Operating MSMPR crystallizers in a closed-loop can allow smaller crystallizer volumes and reduced material requirements for continuous crystallization configurations, but issues with fouling and encrustation can make such setups unfavorable.⁷⁴ A systematic comparison of different processes with and without closed-loop arrangements is required to establish the best process configuration. While the current work does not consider downtime for dealing with fouling issues, operating a closed-loop process will make fouling effects more significant; economic analyses would thus need to consider equipment downtime and additional standby equipment to ensure fully continuous operation of the process. The current work considers processes without closed-loop operation only, in accordance with the experimental demonstrations of the processes with and without solids recycle.^{53,54}

The modeling of continuous crystallization processes using MSMPR crystallizers is a multivariate problem, which requires rigorous mathematical methods to establish the best process configuration. Despite the systematic methods we have used here to investigate the design space for different flowsheet configurations for continuous cyclosporine crystallization, it is imperative to perform mathematical optimizations of such processes to minimize the total costs. Previous work has performed optimization of yield and purity of cyclosporine in a series of MSMPR crystallizers without recycle by varying the temperature and residence time of each crystallizer;⁵³ however, no such optimization study has been performed for the process implementing solids recycle, and no study has yet optimized MSMPR crystallization processes with total costs as the objective function. Such work is imperative to establish economically viable options for continuous crystallization prior to further development.

7. CONCLUSIONS

The present study implements a technoeconomic analysis of two different configurations for the continuous crystallization of cyclosporine: with and without solids recycle, based on experimental demonstrations.^{53,54} A steady-state process model for a cascade of continuous MSMPR crystallizers incorporating population balance equations, crystallization kinetics and process mass balances for different flowsheet permutations allows calculation of yields for different process configurations and operating variables, including varying the number of crystallizers, operating temperatures, total cascade

residence times, API feed concentration and extent and feed point location of recycle streams. The environmental impacts/material efficiencies of different process configurations are evaluated using the widely implemented *E*-factor. Cost analyses using an established methodology for CPM processes allow comparison of the economic viability of the process configurations considered.

The capital expenditures incurred using multiple crystallizers and a gravity-driven separation column as well as high waste handling costs make processes with solids recycle economically inferior to those without recycle. In addition to achieving the lowest total costs, the process using a single crystallizer with no recycle also achieves very low *E*-factors (<10) in comparison to typical pharmaceutical manufacturing processes and other process configurations considered here. Total cost components normalized with respect to total crystallizer volume implemented show the sensitivity of selected residence times on economic analyses and cost comparisons of different process configurations. Due to the complex interplay of operating variables considered here, technoeconomic optimization with respect to total costs is required to establish the optimal process configuration and operating variables for development of the continuous crystallization of cyclosporine. This work demonstrates the value of conducting process modeling studies prior to costly development and scale-up of CPM processes.

AUTHOR INFORMATION

Corresponding Author

*E-mail: D.Gerogiorgis@ed.ac.uk. Tel: +44 131 6517072.

ORCID

Dimitrios I. Gerogiorgis: [0000-0002-2210-6784](https://orcid.org/0000-0002-2210-6784)

Notes

The authors declare no competing financial interest.

ACKNOWLEDGMENTS

The authors gratefully acknowledge the financial support of the Engineering and Physical Sciences Research Council (EPSRC) via a Doctoral Training Partnership (DTP) PhD fellowship awarded to Mr. Samir Diab (Grant No. EP/N509644/1). Tabulated and cited literature data suffice for reproduction of all original process simulation results, and no other supporting research data are stored or required.

NOMENCLATURE AND ACRONYMS

Latin Letters and Acronyms

API	Active pharmaceutical ingredient
B_i	Crystal nucleation rate ($\# \text{ m}^{-3} \text{ min}^{-1}$)
b	Crystal nucleation exponent (—)
BLIC	Battery limits installed costs (GBP)
C_0	Mother liquor API concentration of the fresh feed stream (g mL^{-1})
C_i	API concentration in product magma of MSMPR i (g mL^{-1})
C_i^{sat}	API saturation concentration at T_i (g mL^{-1})
CapEx	Capital expenditure (GBP)
CC	Contingency costs (GBP)
CEPCI	Chemical engineering plant cost index
CPM	Continuous pharmaceutical manufacturing
E	Environmental factor (—)
E_{ag}	Crystal growth activation energy (J mol^{-1})
F_0	Volumetric flow rate of the fresh feed stream (mL min^{-1})

F_i	Volumetric flow rate of stream i (mL min ⁻¹)
f	Correction factor in eq 17
FOB	Free-on-Board Costs (GBP)
G_i	Crystal linear growth rate (m min ⁻¹)
g	Crystal growth exponent (—)
IEC	Installed equipment costs (GBP)
k_{b0}	Pre-exponential factor for crystal nucleation (# m ⁻³ min ⁻¹)
k_{g0}	Pre-exponential factor for crystal growth (m min ⁻¹)
k_v	Crystal volume shape factor (= $\pi/6$ for spherical crystals)
L	Crystal characteristic length (m)
M_i	MSMPR slurry density (g mL ⁻¹)
MAT_{annual}	Annual material costs (GBP y ⁻¹)
MAT_{total}	Total material costs over the plant lifetime (GBP)
MSMPR	Mixed Suspension-Mixed Product Removal
m_{API}	Mass of recovered crystallized API (g min ⁻¹)
m_{waste}	Mass of waste API (g min ⁻¹)
N	Number of MSMPRs in series (—)
n	Exponent in eq 17
n_i	Crystal population density (# m ⁻³ m ⁻¹)
n_i^0	Nuclei population density (# m ⁻³ m ⁻¹)
OBC	Oscillatory Baffled Crystallizer
ODE	Ordinary differential equation
$OpEx_{\text{annual}}$	Annual operating expenditure (GBP y ⁻¹)
$OpEx_{\text{total}}$	Total operating expenditure over the plant lifetime (GBP)
P_j	Equipment purchase cost at capacity j (GBP)
PF	Plug flow
PPI	Process piping and instrumentation costs (GBP)
R	Universal gas constant (= 8.314 J mol ⁻¹ K ⁻¹)
r	Interest rate (%)
S_j	Capacity of equipment (varying units)
T_i	Operating temperature of MSMPR i (°C)
TPPC	Total physical plant cost (GBP)
UW_{annual}	Sum of annual utilities and waste disposal costs (GBP y ⁻¹)
UW_{total}	Total utilities and waste disposal costs over the plant lifetime (GBP)
$UTIL_{\text{annual}}$	Annual utilities costs (GBP y ⁻¹)
V_i	Volume of MSMPR i (mL)
WC	Working capital costs (GBP)
WCC	Working capital and contingency costs (GBP)
x	Clear liquor removal ratio in gravity-driven separation column for continuous crystallization process with solids recycle (—)
$Y_{\text{crystallization}}$	Crystallization yield (%)
$Y_{\text{plantwide,NR/SR}}$	Plantwide API yield for process without/with solids recycle (%)

Greek Letters

ρ_{API}	API solid crystal density (g cm ⁻³)
ρ_{acetone}	Acetone density at T_i (g mL ⁻¹)
τ	Plant operation lifetime (y)
τ_i	Residence time in MSMPR i (h or min)
τ_{total}	Residence time of total crystallizer cascade (h or min)

REFERENCES

(1) Poehlauer, P.; et al. Pharmaceutical Roundtable Study Demonstrates the Value of Continuous Manufacturing in the Design of Greener Processes. *Org. Process Res. Dev.* **2013**, *17*, 1472–1478.

(2) Betz, G.; Junker-Bürgin, P.; Leuenberger, H. Batch And Continuous Processing In The Production Of Pharmaceutical Granules. *Pharm. Dev. Technol.* **2003**, *8*, 289–297.

(3) Plumb, K. Continuous Processing in the Pharmaceutical Industry - Changing the Mind Set. *Chem. Eng. Res. Des.* **2005**, *83*, 730–738.

(4) Calabrese, G. S.; Pissavini, S. From batch to continuous flow processing in chemicals manufacturing. *AIChE J.* **2011**, *57*, 828–834.

(5) Baumann, M.; Baxendale, I. R. The Synthesis of Active Pharmaceutical Ingredients (APIs) Using Continuous Flow Chemistry. *Beilstein J. Org. Chem.* **2015**, *11*, 1194–1219.

(6) Porta, R.; Benaglia, M.; Puglisi, A. Flow Chemistry: Recent Developments in the Synthesis of Pharmaceutical Products. *Org. Process Res. Dev.* **2016**, *20*, 2–25.

(7) Malet-Sanz, L.; Susanne, F. Continuous Flow Synthesis. A Pharma Perspective. *J. Med. Chem.* **2012**, *55*, 4062–4098.

(8) Poehlauer, P.; Manley, J.; Broxterman, R.; Gregertsen, B.; Ridemark, M. Continuous Processing in the Manufacture of Active Pharmaceutical Ingredients and Finished Dosage Forms: An Industry Perspective. *Org. Process Res. Dev.* **2012**, *16*, 1586–1590.

(9) Mascia, S.; et al. End-to-end Continuous Manufacturing of Pharmaceuticals: Integrated Synthesis, Purification, and Final Dosage Formation. *Angew. Chem., Int. Ed.* **2013**, *52*, 12359–12363.

(10) Adamo, A.; et al. On-Demand Continuous-Flow Production of Pharmaceuticals in a Compact, Reconfigurable System. *Science (Washington, DC, U. S.)* **2016**, *352*, 61–67.

(11) GSK. GSK invests a further \$577mil to enhance antibiotic manufacturing facility in Singapore | GSK Singapore (2015). Available at: <http://sg.gsk.com/en-sg/media/press-releases/2015/gsk-invests-a-further-s-77mil-to-enhance-antibiotic-manufacturing-facility-in-singapore/> (accessed 3rd February 2016).

(12) Kuehn, S. E. Janssen Embraces Continuous Manufacturing for Prezista. *Pharmaceutical Manufacturing* (2015). Available at: <http://www.pharmamanufacturing.com/articles/2015/janssen-embraces-continuous-manufacturing-for-prezista/> (accessed 5th October 2016).

(13) Cole, K. P.; et al. Kilogram-scale prexasertib monolactate monohydrate synthesis under continuous-flow CGMP conditions. *Science (Washington, DC, U. S.)* **2017**, *356*, 1144.

(14) Federsel, H.-J. En Route to Full Implementation: Driving the Green Chemistry Agenda in the Pharmaceutical Industry. *Green Chem.* **2013**, *15*, 3105–3115.

(15) Lee, S. L.; et al. Modernizing Pharmaceutical Manufacturing: from Batch to Continuous Production. *J. Pharm. Innov.* **2015**, *10*, 191–199.

(16) Yu, L. X.; et al. Understanding pharmaceutical quality by design. *AAPS J.* **2014**, *16*, 771–83.

(17) Chen, J.; Sarma, B.; Evans, J. M. B.; Myerson, A. S. Pharmaceutical Crystallization. *Cryst. Growth Des.* **2011**, *11*, 887–895.

(18) Randolph, A. D.; Larson, M. A. *Theory of Particulate Processes: Analysis and Techniques of Continuous Crystallization*; Academic Press: 1988.

(19) Eder, R. J. P.; et al. Seed loading effects on the mean crystal size of acetylsalicylic acid in a continuous-flow crystallization device. *Cryst. Res. Technol.* **2011**, *46*, 227–237.

(20) McGlone, T.; et al. Oscillatory Flow Reactors (OFRs) for Continuous Manufacturing and Crystallization. *Org. Process Res. Dev.* **2015**, *19*, 1186–1202.

(21) Alvarez, A. J.; Myerson, A. S. Continuous Plug Flow Crystallization of Pharmaceutical Compounds. *Cryst. Growth Des.* **2010**, *10*, 2219–2228.

(22) Lawton, S.; et al. Continuous crystallization of pharmaceuticals using a continuous oscillatory baffled crystallizer. *Org. Process Res. Dev.* **2009**, *13*, 1357–1363.

(23) Eder, R. J. P.; et al. Continuously Seeded, Continuously Operated Tubular Crystallizer for the Production of Active Pharmaceutical Ingredients. *Cryst. Growth Des.* **2010**, *10*, 2247–2257.

(24) Su, Q.; Benyahia, B.; Nagy, Z. K.; Rielly, C. D. Mathematical Modeling, Design, and Optimization of a Multisegment Multiaddition Plug-Flow Crystallizer for Antisolvent Crystallizations. *Org. Process Res. Dev.* **2015**, *19*, 1859–1870.

- (25) Vetter, T.; Burcham, C. L.; Doherty, M. F. Regions of attainable particle sizes in continuous and batch crystallization processes. *Chem. Eng. Sci.* **2014**, *106*, 167–180.
- (26) Ridder, B. J.; Majumder, A.; Nagy, Z. K. Parametric, Optimization-Based Study on the Feasibility of a Multisegment Antisolvent Crystallizer for in Situ Fines Removal and Matching of Target Size Distribution. *Ind. Eng. Chem. Res.* **2016**, *55*, 2371–2380.
- (27) Mullin, J. W. *Crystallization*; Butterworth-Heinemann: 2001.
- (28) Quon, J. L.; et al. Continuous Crystallization of Aliskiren Hemifumarate. *Cryst. Growth Des.* **2012**, *12*, 3036–3044.
- (29) Power, G.; et al. Design and optimization of a multistage continuous cooling mixed suspension, mixed product removal crystallizer. *Chem. Eng. Sci.* **2015**, *133*, 125–139.
- (30) Acevedo, D.; et al. Evaluation of mixed suspension mixed product removal crystallization processes coupled with a continuous filtration system. *Chem. Eng. Process.* **2016**, *108*, 212–219.
- (31) Timothy, M. B.; et al. Reactors and methods for processing reactants therein. *World Pat.* 023 515 (2009).
- (32) Ferguson, S.; Morris, G.; Hao, H.; Barrett, M.; Glennon, B. Characterization of the anti-solvent batch, plug flow and MSMR crystallization of benzoic acid. *Chem. Eng. Sci.* **2013**, *104*, 44–54.
- (33) Ferguson, S.; et al. Use of continuous MSMR crystallization with integrated nanofiltration membrane recycle for enhanced yield and purity in API crystallization. *Cryst. Growth Des.* **2014**, *14*, 617–627.
- (34) Vartak, S.; Myerson, A. S. Continuous Crystallization with Impurity Complexation and Nanofiltration Recycle. *Org. Process Res. Dev.* **2017**, *21*, 253–261.
- (35) Sang-Il Kwon, J.; Nayhouse, M.; Orkoulas, G.; Christofides, P. D. Crystal shape and size control using a plug flow crystallization configuration. *Chem. Eng. Sci.* **2014**, *119*, 30–39.
- (36) Kwon, J. S.-I.; Nayhouse, M.; Orkoulas, G.; Christofides, P. D. Enhancing the Crystal Production Rate and Reducing Polydispersity in Continuous Protein Crystallization. *Ind. Eng. Chem. Res.* **2014**, *53*, 15538–15548.
- (37) Nayhouse, M.; et al. Modeling and control of ibuprofen crystal growth and size distribution. *Chem. Eng. Sci.* **2015**, *134*, 414–422.
- (38) Lai, T.-T. C.; Ferguson, S.; Palmer, L.; Trout, B. L.; Myerson, A. S. Continuous Crystallization and Polymorph Dynamics in the L-Glutamic Acid System. *Org. Process Res. Dev.* **2014**, *18*, 1382–1390.
- (39) Lai, T.-T. C.; et al. Control of Polymorphism in Continuous Crystallization via Mixed Suspension Mixed Product Removal Systems Cascade Design. *Cryst. Growth Des.* **2015**, *15*, 3374–3382.
- (40) Farmer, T. C.; Carpenter, C. L.; Doherty, M. F. Polymorph selection by continuous crystallization. *AIChE J.* **2016**, *62*, 3505–3514.
- (41) Vetter, T.; Burcham, C. L.; Doherty, M. F. Separation of conglomerate forming enantiomers using a novel continuous preferential crystallization process. *AIChE J.* **2015**, *61*, 2810–2823.
- (42) Steendam, R. R. E.; ter Horst, J. H. Continuous Total Spontaneous Resolution. *Cryst. Growth Des.* **2017**, *17*, 4428–4436.
- (43) Teoh, S. K.; Rathi, C.; Sharratt, P. Practical Assessment Methodology for Converting Fine Chemicals Processes from Batch to Continuous. *Org. Process Res. Dev.* **2016**, *20*, 414–431.
- (44) Mesbah, A.; Paulson, J. A.; Lakerveld, R.; Braatz, R. D. Model Predictive Control of an Integrated Continuous Pharmaceutical Manufacturing Pilot Plant. *Org. Process Res. Dev.* **2017**, *21*, 844–854.
- (45) Besenhard, M. O.; Hohl, R.; Hodzic, A.; Eder, R. J. P.; Khinast, J. G. Modeling a seeded continuous crystallizer for the production of active pharmaceutical ingredients. *Cryst. Res. Technol.* **2014**, *49*, 92–108.
- (46) Yang, Y.; Nagy, Z. K. Advanced control approaches for combined cooling/antisolvent crystallization in continuous mixed suspension mixed product removal cascade crystallizers. *Chem. Eng. Sci.* **2015**, *127*, 362–373.
- (47) Yang, Y.; Nagy, Z. K. Combined Cooling and Antisolvent Crystallization in Continuous Mixed Suspension, Mixed Product Removal Cascade Crystallizers: Steady-State and Startup Optimization. *Ind. Eng. Chem. Res.* **2015**, *54*, 5673–5682.
- (48) Park, K.; Kim, D. Y.; Yang, D. R. Operating Strategy for Continuous Multistage Mixed Suspension and Mixed Product Removal (MSMPR) Crystallization Processes Depending on Crystallization Kinetic Parameters. *Ind. Eng. Chem. Res.* **2016**, *55*, 7142–7153.
- (49) Su, Q.; Nagy, Z. K.; Rielly, C. D. Pharmaceutical crystallisation processes from batch to continuous operation using MSMPR stages: Modelling, design, and control. *Chem. Eng. Process.* **2015**, *89*, 41–53.
- (50) Nussenblatt, R. B.; Palestine, A. G. Cyclosporine: Immunology, pharmacology and therapeutic uses. *Surv. Ophthalmol.* **1986**, *31*, 159–169.
- (51) Groisser, D. S.; Griffiths, C. E.; Ellis, C. N.; Voorhees, J. J. A review and update of the clinical uses of cyclosporine in dermatology. *Dermatol. Clin.* **1991**, *9*, 805–17.
- (52) Alvarez, A. J.; Singh, A.; Myerson, A. S. Crystallization of cyclosporine in a multistage continuous MSMPR crystallizer. *Cryst. Growth Des.* **2011**, *11*, 4392–4400.
- (53) Li, J.; Lai, T. C.; Trout, B. L.; Myerson, A. S. Continuous Crystallization of Cyclosporine: the Effect of Operating Conditions on Yield and Purity. *Cryst. Growth Des.* **2017**, *17*, 1000–1007.
- (54) Li, J.; Trout, B. L.; Myerson, A. S. Multistage Continuous Mixed-Suspension, Mixed-Product Removal (MSMPR) Crystallization with Solids Recycle. *Org. Process Res. Dev.* **2016**, *20*, 510–516.
- (55) Wong, S. Y.; Tatusko, A. P.; Trout, B. L.; Myerson, A. S. Development of continuous crystallization processes using a single-stage mixed-suspension, mixed-product removal crystallizer with recycle. *Cryst. Growth Des.* **2012**, *12*, 5701–5707.
- (56) Fujiwara, M.; Nagy, Z. K.; Chew, J. W.; Braatz, R. D. First-principles and direct design approaches for the control of pharmaceutical crystallization. *J. Process Control* **2005**, *15*, 493–504.
- (57) Yu, L. Applications of process analytical technology to crystallization processes. *Adv. Drug Delivery Rev.* **2004**, *56*, 349–369.
- (58) Schaber, S. D.; et al. Economic Analysis of Integrated Continuous and Batch Pharmaceutical Manufacturing: A Case Study. *Ind. Eng. Chem. Res.* **2011**, *50*, 10083–10092.
- (59) Jolliffe, H. G.; Gerogiorgis, D. I. Plantwide Design and Economic Evaluation of Two Continuous Pharmaceutical Manufacturing (CPM) Cases: Ibuprofen and Artemisinin. *Comput. Chem. Eng.* **2016**, *91*, 269–288.
- (60) Jolliffe, H. G.; Gerogiorgis, D. I. Technoeconomic Optimization of a Conceptual Flowsheet for Continuous Separation of an Analgesic Active Pharmaceutical Ingredient (API). *Ind. Eng. Chem. Res.* **2017**, *56*, 4357–4376.
- (61) Jolliffe, H. G.; Gerogiorgis, D. I. Technoeconomic optimization and comparative environmental impact evaluation of continuous crystallisation and antisolvent selection for artemisinin recovery. *Comput. Chem. Eng.* **2017**, *103*, 218–232.
- (62) Diab, S.; Gerogiorgis, D. I. Process Modeling, Simulation, and Technoeconomic Evaluation of Separation Solvents for the Continuous Pharmaceutical Manufacturing (CPM) of Diphenhydramine. *Org. Process Res. Dev.* **2017**, *21*, 924–946.
- (63) Diab, S.; Gerogiorgis, D. I. Technoeconomic Analyses of Separation Processes for Continuous Pharmaceutical Manufacturing: Assessing Process Performance, Material Efficiency and Economic Viability. *Chim. Oggi* **2017**, *35*, 14–17.
- (64) Myerson, A. S. *Handbook of industrial crystallization*; Butterworth-Heinemann: 2002.
- (65) Yang, Y.; Nagy, Z. K. Model-Based Systematic Design and Analysis Approach for Unseeded Combined Cooling and Antisolvent Crystallization (CCAC) Systems. *Cryst. Growth Des.* **2014**, *14*, 687–698.
- (66) Atwood, J. L. Separation of Active Pharmaceutical Ingredients (APIs) from excipients in pharmaceutical formulations. *Cryst. Growth Des.* **2015**, *15*, 2874–2877.
- (67) Sheldon, R. A. Fundamentals of Green Chemistry: Efficiency in Reaction Design. *Chem. Soc. Rev.* **2012**, *41*, 1437–1451.
- (68) Constable, D. J. C.; Curzons, A. D.; Cunningham, V. L. Metrics to green chemistry - which are the best? *Green Chem.* **2002**, *4*, 521–527.

(69) Morris, G.; et al. Estimation of Nucleation and Growth Kinetics of Benzoic Acid by Population Balance Modeling of a Continuous Cooling Mixed Suspension, Mixed Product Removal Crystallizer. *Org. Process Res. Dev.* **2015**, *19*, 1891–1902.

(70) Woods, D. R. *Rules of Thumb in Engineering Practice*; Wiley: 2007.

(71) ProMinent. Solenoid Driven Metering Pumps (2015). Available at: <https://www.prominent.co.uk/en/Products/Products/Metering-Pumps/Solenoid-Driven-Metering-Pumps/pg-solenoid-driven-metering-pumps.html> (accessed 8th March 2016).

(72) Couper, J. R. *Process Engineering Economics*; CRC Press: 2003.

(73) Ritter, S. K. Reducing Environmental Impact of Organic Synthesis. *Chem. Eng. News* **2013**, *91*, 22–23.

(74) Powell, K. A.; Saleemi, A. N.; Rielly, C. D.; Nagy, Z. K. Monitoring Continuous Crystallization of Paracetamol in the Presence of an Additive Using an Integrated PAT Array and Multivariate Methods. *Org. Process Res. Dev.* **2016**, *20*, 626–636.